16.1

A CLIMATOLOGY OF LARGE-SCALE NORTH PACIFIC CYCLONES AND THEIR PREDICTABILITY

Linda M. Keller* and Michael C. Morgan

University of Wisconsin – Madison
Madison, Wisconsin

1. INTRODUCTION

It has been long recognized that there are certain anomalous weather patterns that persist on time scales longer than typical synoptic-scale variability. These events, which include blocking, teleconnection patterns, and other realizations of persistent flow anomalies (e.g., Dole, 1986; Dole and Black, 1990) are associated with significant and important changes in the extratropical general circulation and related weather sequences. It is widely believed that predictability in the medium to extended range is diminished during the development of these low-frequency flow patterns, and it has been observed that during the occurrence of certain of these atmospheric flows, predictability is enhanced.

Palmer (1988) and Molteni and Palmer (1993) have demonstrated the dependence of predictability on the phase of the Pacific-North American (PNA) teleconnection pattern and that the differences in predictability could be related to changes in the characteristics of the most rapidly growing perturbations of the observed flow.

The episodic large-scale cyclogenesis events (LSCs, Black and Dole, 1993) over the North Pacific are a particularly interesting class of a low-frequency weather pattern that potentially has a significant impact on predictability over North America.

In this study, the results of an updated climatology of these events are presented. In section 2, the data used and the methodology are described. Initial results of the climatology of the events and composite evolution are found in section 3. Future research directions are briefly described in section 4.

2. DATA AND METHODOLOGY

The data set used in the initial phase of this work consists of National Center for Environmental Prediction (NCEP) reanalysis data (Kalnay et al. 1996) for 500 hPa geopotential height and sea level pressure. The period covered in this study is the cold season (November through March) for 1977-78 through 2002-03. The reanalysis data are global on a 2.5 X 2.5 degree grid available every 6 hours. For the purposes of this study, the meridional extent of the data has been reduced to 2.5S - 90N.

Twenty-five years of the study period (1977-78 - 2001-02) were used to calculate the climatology. The 25 values at each time period were averaged to form the climatology, and this calculation was performed at each grid point. The geopotential height anomalies were calculated by subtracting the climatology from the original data for each time period and at each grid point. The time series of anomalies at each grid point were filtered with a 151 point Lanczos filter (Duchon, 1979) with a cut off frequency of 10 days. The height anomalies were normalized by a scale factor that was inversely proportional to the sine of the latitude (Dole and Gordon, 1983).

Following Dole and Gordon (1983), the filtered time series at each grid point was examined for each winter season for negative 500 hPa height anomalies which were greater than 100 m and for at least 10 days. Examination of the frequency of occurrence of these anomaly events in the North Pacific showed two areas of maximum activity (Fig. 1).

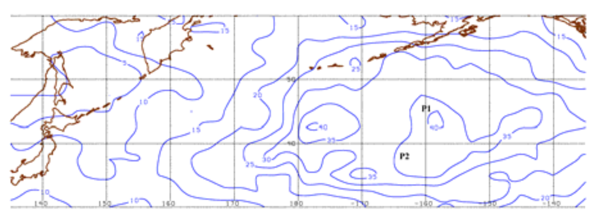

Fig.1 Number of times in November to March periods from 1977 through 2002 that the filtered 500 hPa geopotential height is at least 100 m below climatology for at least 10 days.

*Corresponding author address: Linda M. Keller, University of Wisconsin – Madison, Department of Atmospheric and Oceanic Sciences, 1225 W. Dayton Street, Madison, Wisconsin 53706
e-mail: lmkeller@wisc.edu

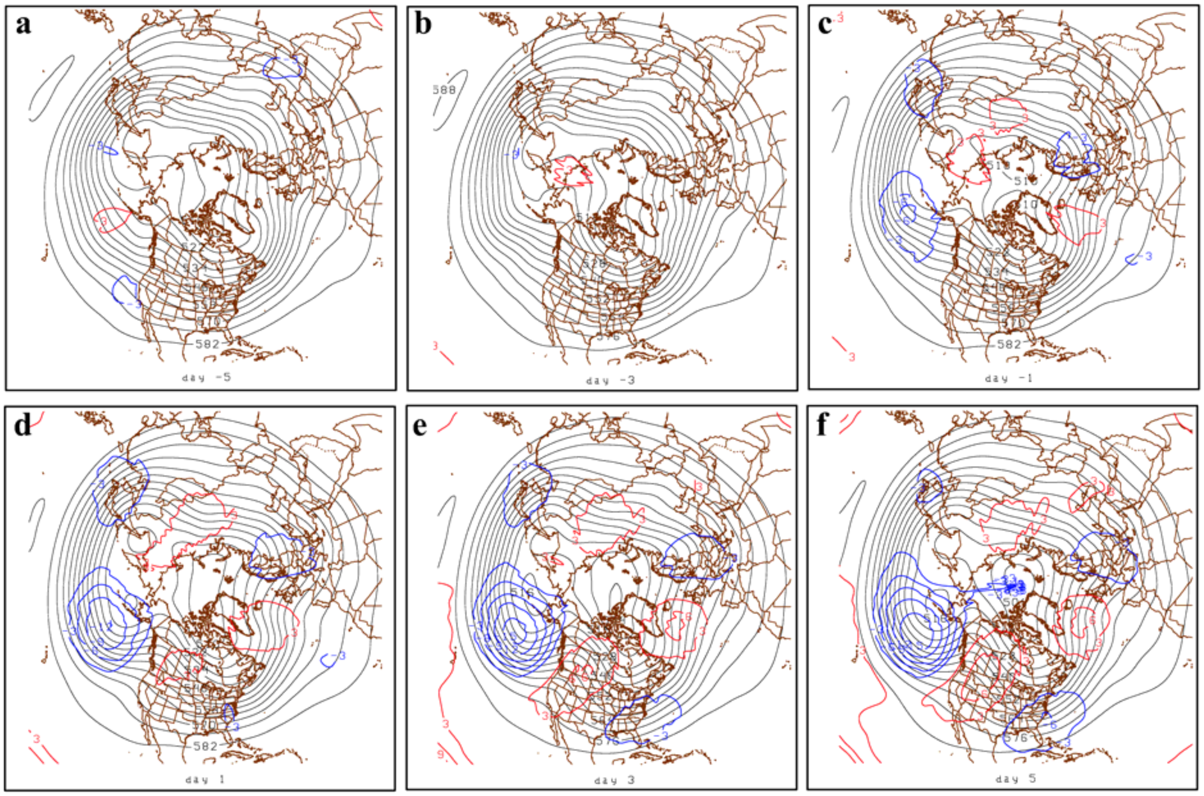

Fig. 2 Evolution of composite 500 hPa geopotential heights (black, interval 6 dam) and geopotential height anomalies (color contours, interval 3 dam) associated with events located with KP1 at (a) Day-5, (b) Day-3, (c) Day-1, (d) Day+1, (e) Day+3, and (f) Day+5.

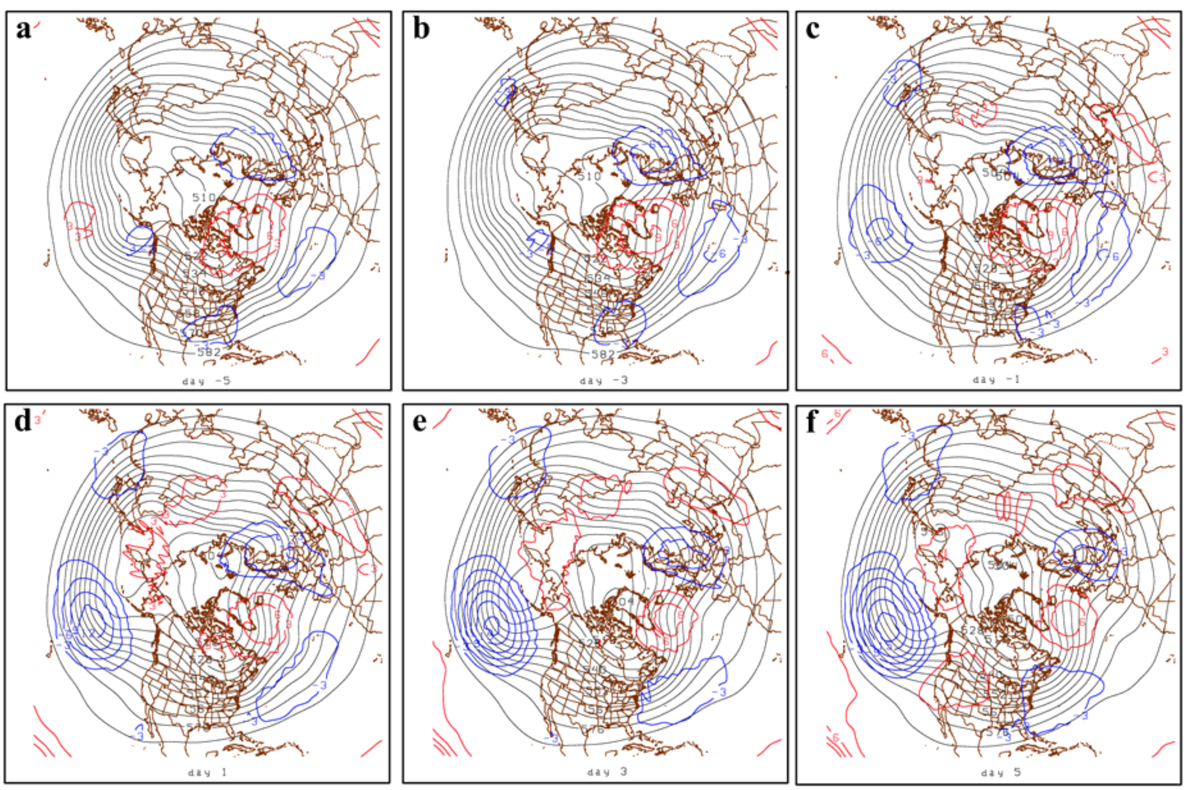

Fig. 3 As in Fig. 2, except for KP1.

Variations in the North Pacific sea level pressure exhibit quasi-decadal shifts in magnitude and position of the Aleutian Low. The shift in 1976-77 has been well documented. The possibility of another 'regime shift' in 1988-89 has been explored by Yasunaka and Hanawa (2002). To examine the effect of this possible change in background state on the climatology of the LSCs, the events were partitioned into those occurring before November, 1988 and those occurring after this time. The events before 1988 are located mainly north of 40N and extend from 180 to 150W in an arc across the central Pacific. The events from 1988 on are found primarily south of 40N and centered between 180 and 160W. Grid points were chosen at 160W, 45N and 162.5W, 37.5N to represent these areas. Henceforth, these points will be referred to as *key points* 1 (KP1) and 2 (KP2) respectively. Following the criteria above, 40 events were identified at the first key point and 38 events were identified at the second key point.

Composited hemispheric height and sea level pressure analyses were produced for events identified at the two key points. The onset time for each event was defined as the time when the 500 hPa height anomaly at the representative grid point dropped below -100 m. The composites were made for 15 days (60 time periods) to study the evolution of the events. The composites were started 5 days before the onset of the event, so the onset occurs at day 6/0000 in the 15 day period.

3. DESCRIPTION OF COMPOSITE ANALYSES

*a) Initial anomaly structure and evolution for KP*1

The composite evolution of the 500 hPa anomalies and full geopotential height fields for KP1 are shown in Fig. 2 for days -5, -3, -1, +1, +3, and +5 respectively. Five days prior to onset of the event (Fig. 2a), over the hemisphere, the 500 hPa height field characterized by the composite reveals relatively weak geopotential height anomalies over the Pacific, with anomalously high heights (red lines) near KP1 straddled by low heights (blue lines) off the eastern Asian and western North American coasts. During the subsequent three days (Figs. 2b and 2c), the anomalously high heights near KP1 decrease, while the negative height anomaly increases in amplitude over the western Pacific and propagates eastward into the central Pacific. Upstream of the region, over the southern Japanese islands and South Korea, a region of negative height anomalies develops and persists throughout the duration of the composite event. Much further downstream, over the Atlantic, south of Greenland, a positive height anomaly has begun to grow. This feature amplifies over the next several days and also persists throughout the duration of the event.

By Day+1 (Fig. 2d), the composite height anomalies over KP1 decrease to 120 m below average while downstream, positive height anomalies begin to grow over western North America with the largest anomalies over Alberta and Saskatchewan. In addition, negative height perturbations begin to amplify over the southeastern United States in a region centered over the Carolinas. The development of this series of height anomalies is reminiscent of a downstream development scenario. The pattern of geopotential height anomalies established by Day+1 essentially remain stationary but amplify through Day+5 (Fig. 2f). Following this time, the anomalies remain steady in amplitude or slowly weaken.

b) Initial anomaly structure and evolution for KP2

In contrast to the composite Day-5 hemispheric geopotential height anomaly pattern described above for KP1, the anomaly pattern at Day-5 for KP2 shows a significant, well-established dipole height anomaly pattern over the central Atlantic, with a positive (in excess of 60 m) geopotential height anomaly south of Greenland and a somewhat weaker, negative height anomaly to the south of the positive anomaly (Fig. 3a). Throughout the composite evolution, the northern most part of this dipole remains nearly stationary with slight fluctuations in intensity.

Over the central Pacific, a positive height anomaly in excess of 30 m is present at Day-5 (Fig. 3a). This anomaly pattern rapidly collapses and is replaced by a negative geopotential height anomaly (in excess of 60 m) by Day-1 (Fig. 3c). This anomaly subsequently amplifies in place. In further contrast to the anomaly field associated with KP1, the amplification of the downstream ridge over western North America, does not really commence until about Day+2 (Fig. 3e). The maximum in this height anomaly, located over northern Utah, is south of the corresponding maximum found in KP1.

Finally, the negative height anomaly that is found downstream just east of the United States southern New England coast, appears to arise from a retrogression of the Day-5 negative height anomaly over the central Atlantic, rather than a downstream development from the west.

c) Mature anomaly structure for KP1 and KP2

By Day+9.5 (Fig. 4), differences between the anomaly patterns associated with composites for both KP1 and KP2 still exist. Most significantly, the amplitudes of the geopotential anomalies associated with KP2 are much larger over much of the Northern Hemisphere. In particular the Pacific negative height anomaly and immediate downstream positive height anomaly are much more robust, as are the height anomalies over the central and far eastern Atlantic.

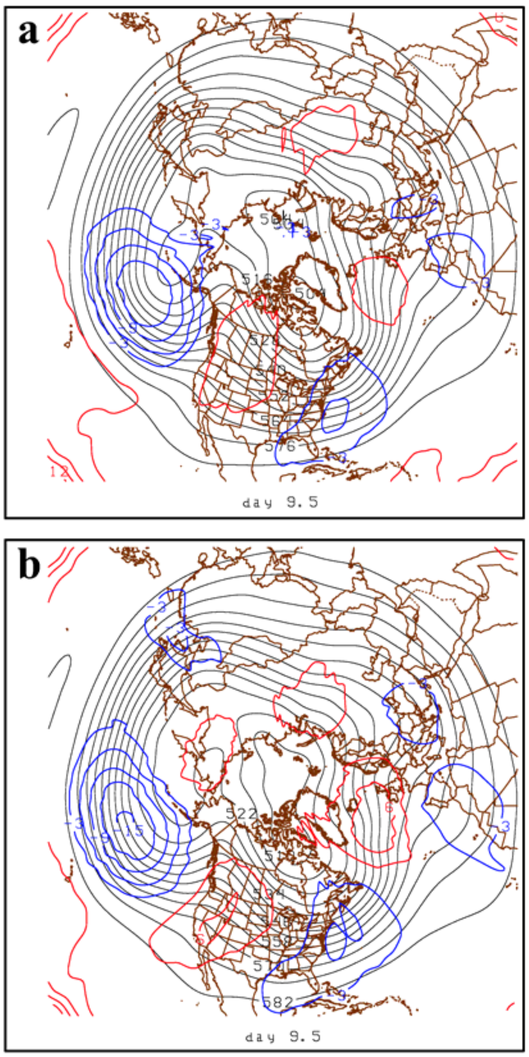

Fig. 4. Day+9.5 composite geopotential height and geopotential height anomalies for (a) KP1 and (b) KP2.

d) Hovmoeller diagrams for KP1 and KP2

Many of the features described in the composite evolutions in the proceeding sections are readily seen in the Hovmoeller diagrams constructed for the composite anomalies for KP1 (Fig. 5a) and KP2 (Fig. 5b). The Hovmoeller diagrams were constructed by meridionally averaging the composite anomaly fields +/-10^{o} latitude of the latitude of the KP. (The results shown here are relatively insensitive to the meridional extent of the averaging performed.) The differences in the initial development of the anomaly fields at the key points are highlighted by the apparent ‘propagation’ and subsequent rapid development of a negative height anomaly from longitude 150E towards the longitude of KP1 between Day-5 and Day-1.5 This development is in marked contrast to the “in place development” of the negative height anomaly for KP2 wherein the anomaly field appears to abruptly change sign and grow soon after Day-4. The development of this negative height anomaly may be associated with the southward migration of the polar vortex over the North Pacific.

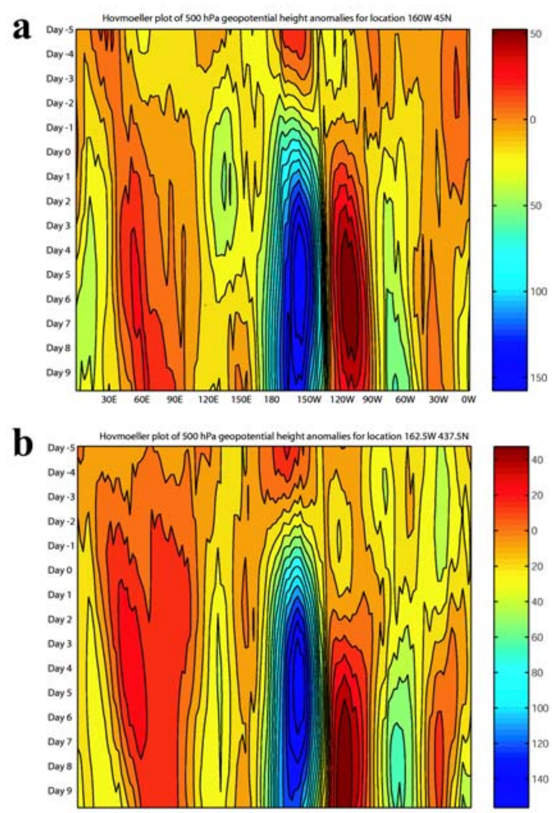

Fig. 5 Hovmoeller diagram of 500 hPa composite height anomalies (m) for (a) KP1 and (b) KP2.

Downstream differences are also apparent. For KP1, the western North American ridge is seen to grow rapidly after the central Pacific negative anomaly begins amplifying with both anomalies reaching their (meridionally averaged) maximum amplitudes within half a day of Day+6. For KP2, there is a lag before the development of the downstream ridge (positive height anomaly) by as much as 5 days.

Further downstream, over the eastern US and western Atlantic the development of the negative height anomaly for KP2 is, in fact, associated with a westward movement (between Day+1 and Day+3) of the negative height anomaly located at longitude 30W at Day-5.

e) Mean sea level pressure changes

Differences in mean-sea level pressure between Day+9.5 and Day-5 (Fig. 6) reveal sea level pressure decreases of as much as 18 hPa. The pressure changes are of large-scale for both composites, but the largest spatial coverage of decreases in sea level pressure are observed for KP2.

Significant pressure changes are not confined to only the Pacific basin. Notable pressure increases are also observed over Europe and western Asia for both composites.

4. FUTURE WORK

After establishing a climatology of these events, the next phase of this work will be to identify the precursors to these events using adjoint-derived forecast sensitivities and to construct a climatology of the predictability of the flow prior to and during the occurrence of these LSCs. The predictability will be assessed by computing the amplification factors of the leading singular vectors of the flow.

5. REFERENCES

Black, R. X., and R. M. Dole, 1993: The dynamics of large-scale cyclogenesis over the North Pacific Ocean. *J. Atmos. Sci.*, **55**, 3159-3175.

Duchon, C. E., 1979: Lanczos filtering in one and two dimensions. *J. Appl. Meteor.*, **18**, 1016-1022.

Dole, R. M., 1986: Life cycles of persistent anomalies, Part 1: Evolution of 500 mb height fields. *Mon. Wea. Rev.*, **117**, 177-211.

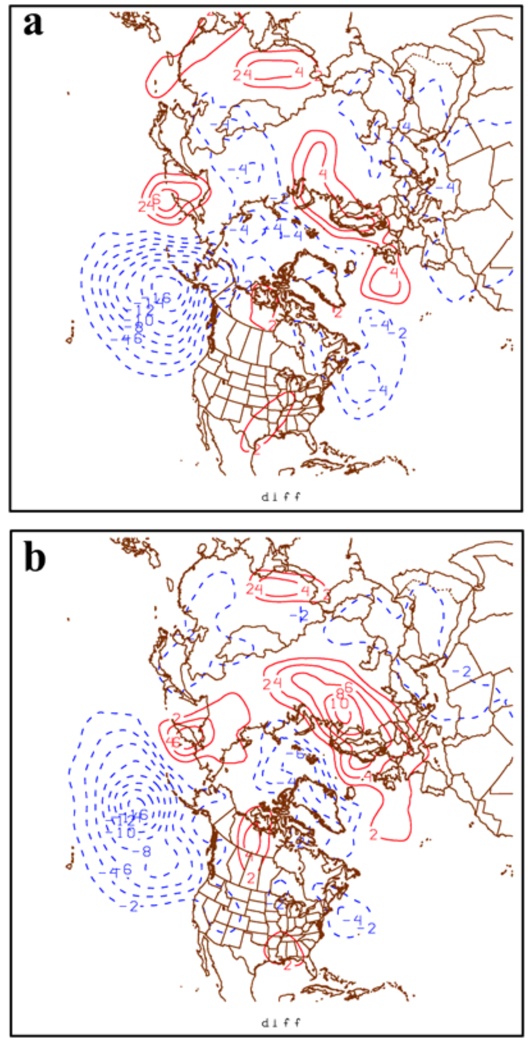

Fig. 6 Mean sea level pressure changes (interval 2hPa) between Day+9.5 and Day-5 for (a) KP1 and (b) KP2.

Dole, R. M. and N. D. Gordon, 1983: Persistent anomalies of the extratropical North Hemisphere wintertime circulation: Geographical distribution and regional persistence characteristics. *Mon. Wea. Rev.*, **111**, 1567-1586.

Dole, R. M. and R. X. Black, 1990: Life cycles of persistent anomalies, Part II: The development of persistent negative height anomalies over the North Pacific Ocean. *Mon. Wea. Rev.*, **118**, 824-846.

Kalnay, E. et al., 1996: The NCEP/NCAR 40-year reanalysis project. *Bull. Amer. Meteor. Soc.*, **77**, 437-471.

Molteni, F., and T. N. Palmer, 1993: Predictability and finite-time instability of the northern winter circulation. *Quart. J. Roy. Meteor. Soc.*, **119**, 269-298.

Palmer, T. N., 1988: Medium and extended range predictability, and the stability of the PNA mode. *Quart. J. Roy. Meteor. Soc.*, **114**, 691-713.

Yasunaka, S. and K. Hanawa, 2002: Regime shifts in the Northern Hemisphere SST field. *J. Met. Soc. Japan*, **80**, 119-135.

Acknowledgements

This work is supported by the National Science Foundation Grant ATM-0121186.